CV ref C25

14th Nuclear Simulation Symp, Pinawa, 1988

PREDICTION OF PRESSURIZER TRANSIENTS BY THE IDRIFF TWO-PHASE SIMULATION CODE

R. Sollychin[1], J.S. Chang and W.J. Garland

Dept. of Engineering Physics
McMaster University
Hamilton, Ontario, Canada
L8S 4M1

ABSTRACT

A small scale pressurizer made of a glass tank and its associated systems were set up to simulate the behaviour of a nuclear power plant pressurizer. A version of the IDRIFF two-phase simulation code is specially designed to simulate the experiments such that any particular pressurizer phenomena of interest can be calculated in detail without the necessity of performing unnecessary detailed calculations on the other aspects. The code consists of two major model components: (1) lumped formulation for the fluid conservation equations and the equation of state; (2) sets of one-dimensional drift-flux equation and the equation of state written in differential forms.

The study on three types of pressurizer transients is reported in the present paper. They are: (a) transients following a step-wise change in heater power; (b) transients following step-wise change in steam bleed valve opening; and (c) transients following sudden and short-lived outsurge and insurge. The results of the simulation are in good agreement with experimental measurements. By analyzing the effect of a single parameter while isolating the effect of others, several useful insights on the behaviour of the pressurizer were obtained.

---

[1] Present address: Chalk River Nuclear Laboratories
Chalk River, Ontario
Canada, K0J 1J0

1. INTRODUCTION

Many pressurizer models are reported in the literature or currently used in the nuclear industry. Examples are those developed by Gorman [1], Nahavandi and Makkenchery [2], and Baggoura and Martin [3]. In most of them, the thermodynamic state(s) of the fluid in the pressurizer is pre-assumed. Mathematical models are then set up based on this assumption. The models are usually adequate in predicting pressurizer behaviour qualitatively. However, inconsistent performance of the models for different power plant transients is generally reported [4,5]. It is believed that the major drawback of these pressurizer models is due to the lack of understanding on the detailed physical phenomena in the pressurizer. There has been a renewed interest in the systematic study of local thermalhydraulic phenomena in the pressurizer. An example is the work by Griffith and his coworkers [5], in which phenomena such as heat transfer to walls, interface mass transfer and stratification of insurge fluid have been investigated. Simulation of the behaviour of a pressurizer using a sophisticated system code has also been attempted [6]. In the present study of the pressurizer, problems such as the effect of boundary conditions, pressure, temperature and void fraction axial profiles, and quasi-steady-state flow-patterns are investigated as well.

The study is based on both experimental investigations as well as numerical simulation. A McMaster 1:20 scale pressurizer experimental loop was used to conduct the experimental investigation. The facility and test procedure during the experiment is described in Section 2.

A highly flexible simulation tool is needed such that any physical phenomena in the pressurizer can be simulated and that if a particular phenomena (or a parameter) is to be investigated, detailed information about the phenomena (or parameter) can be obtained without the necessity of performing unnecessary detailed calculations on other aspects as well. A version of the IDRIFF two-phase simulation code [7] was specially designed to meet this requirement and was used to simulate the phenomena observed and measured in the experiment. Detail description of the IDRIFF code has been presented elsewhere [7,8] and will briefly be summarized in Section 3.

The current study of the pressurizer consists of two parts: The first part is the investigation of the pressurizer quasi-steady-state phenomena, including the flow patterns of fluids in the pressurizer. The preliminary result of this part of study has been reported [7]. A follow-up analysis of the result, including transitions of the flow patterns will be presented shortly [9]. The second part of the study is the investigation of the single-parameter-perturbation types of transients in the pressurizer. Three types of these transients are simulated in the experimental loop and by the IDRIFF code: (a) transients following a step-change in heater power; (b) transients following a step-change in steam-bleed valve opening; and (c) transients following sudden and short-lived outsurge and insurge. The results of the study on these three types of transients will be presented in Section 4,5 and 6 of this paper respectively.

2. EXPERIMENTAL FACILITY AND TEST PROCEDURE

The McMaster pressurizer experimental loop is schematically shown in Figure 1. The loop mainly consists of a test-pressurizer and a simulated primary heat transport system (PHTS). Experimental observations are mainly concentrated on the test-pressurizer. A surge line is installed from the bottom of the test-pressurizer and is connected to the simulated PHTS. The latter is used to provide fluid at various pressure and temperature such that when a control valve on the surge-line is opened, various conditions of insurge and outsurge can be created as boundary conditions to the test-pressurizer.

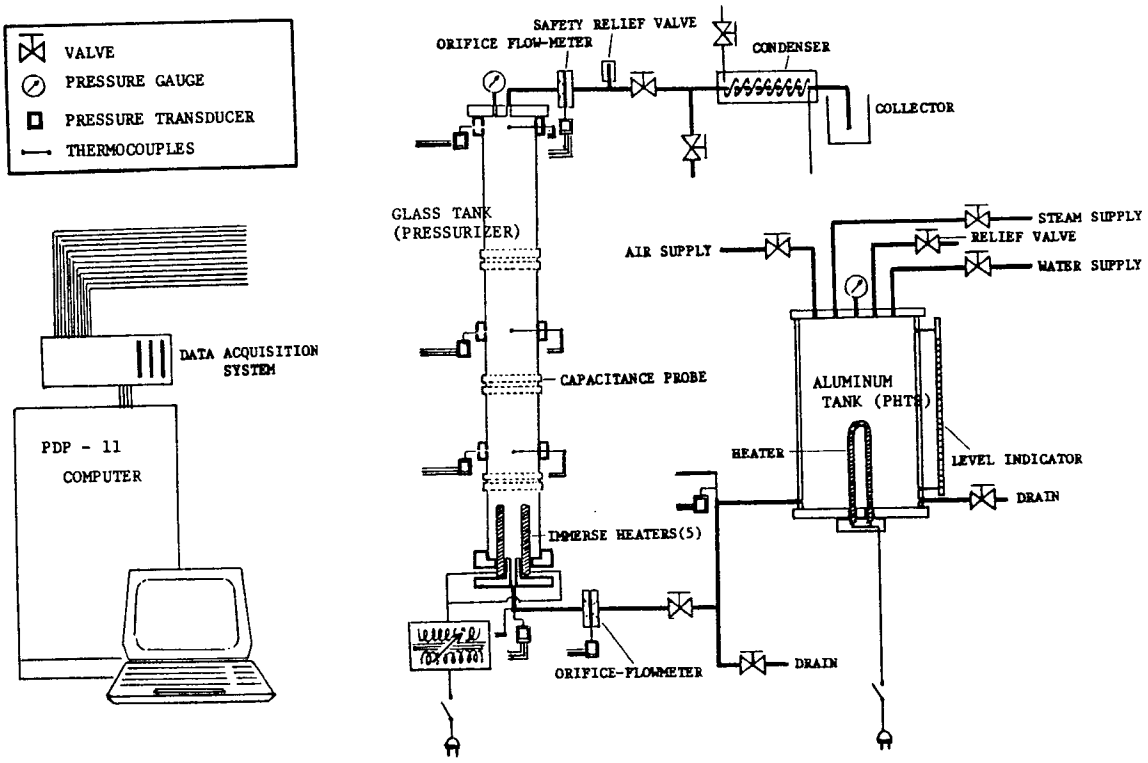

FIGURE 1. Schematic of McMaster Pressurizer Experimental Loop

The test pressurizer itself is a glass made cylindrical tank with an inside-diameter of 5.1 cm and a height of about 66 cm. Five immersion type electrical heaters are installed at the bottom of the tank. The heat generated from the heaters can be adjusted using a variable transformer to a maximum of 1 Kw. A control valve and an adjustable relief valve on top of the tank are used to control a steam-bleed flow and hence to control the steam pressure in the pressurizer. Three pressure transducers, three thermocouples and three capacitance void transducers are installed on the test pressurizer. The capacitance transducers are used to measure void-fraction of the fluid. Orifice flow meters are installed at the steam-bleed line and the surge line to measure flow. Using a data acquisition system, experimental data are processed in a PDP-11 computer.

The objective of the transient experiment is to observe the effect of the perturbation in terms of changes in the heater power, steam-bleed and surge-flow on the pressurizer, initially being at some quasi-steady-state. The procedure of the transient experiment is described as follows:

By closing the surge-line valve and by controlling the heater power, liquid level and steam pressure to some constant values, the pressurizer fluid eventually reaches a quasi-steady-state, in which heat input from the heater is approximately balanced by the sum of heat loss through pressurizer tank wall and energy carried out by the steam-bleed flow. The fluid condition in the pressurizer is adjusted such that the initial condition is approximated by one of four prescribed quasi-steady-states as listed in Table 1.

TABLE 1. Quasi-Steady-State Initial Conditions Setting Matrix

Quasi-Steady-State	Heaters Power (Watt)	Steam Bld. Valve Opening (%)	Steam Pressure (kPa)	Liquid Level (cm)
1	~160	5-15	105-140	20-30
2	~250	10-20	120-155	
3	~475	20-30	140-210	
4	~350	15-25	130-170	

The four prescribed quasi-steady-state initial conditions basically cover a practical range of all quasi-steady-state conditions that can be simulated in the test-pressurizer [7,9].

The actual transient experiment is initiated by introducing a perturbation to one of the three pressurizer control parameters: heater power, steam-bleed flow and surge line flow. The pressurizer reacts to the change and eventually reaches another quasi-steady-state. The transient of the pressurizer from the initial quasi-steady-state to the final quasi-steady-state is recorded.

The perturbation in heater power is introduced by adjusting the variable transformer on a step change basis. The opening of the steam-bleed valve is changed according to a step function as well. However, the resulted change in the actual steam-bleed flow is almost of a pulse function type due to the change in the steam pressure. For example, as the steam-bleed valve opening is suddenly increased, steam-bleed flow increases rapidly. This causes the steam pressure to decrease. As the pressure drop across the steam-bleed valve declines, steam-bleed flow decreases rapidly. The surge flow is also of pulse function nature. This is achieved by rapid opening of the surge-line valve for a short period of time (approx. 8 s). Prior to the opening of the valve, the thermodynamic condition in the simulated PHTS is adjusted

accordingly. Depending upon the pressure difference across the surge line, various insurge or outsurge can be performed.

3. IDRIFF CODE AND SIMULATION PROCEDURE

The mathematical models of the IDRIFF (Integrated Drift-Flux Formulation) two-phase simulation code will briefly be described within the context of the current study, that is, the modelling of the pressurizer.

The basic structure of the IDRIFF code is a set of fluid mass, energy, and volume balance equations and the equation of state, written in lumped (integrated) form. (See Equation A1 to A5, and A10, A11 in Appendix A). As shown in Figure 2, the pressurizer is divided into two control volumes, with the one dominated by the gas phase geometrically above the liquid phase dominated one. The lumped formulation is then applied to each of the control volumes. The size of both control volumes is dynamically adjusted according to the calculation of swelling or shrinking in the lower control volume, which is dominated by the liquid phase.

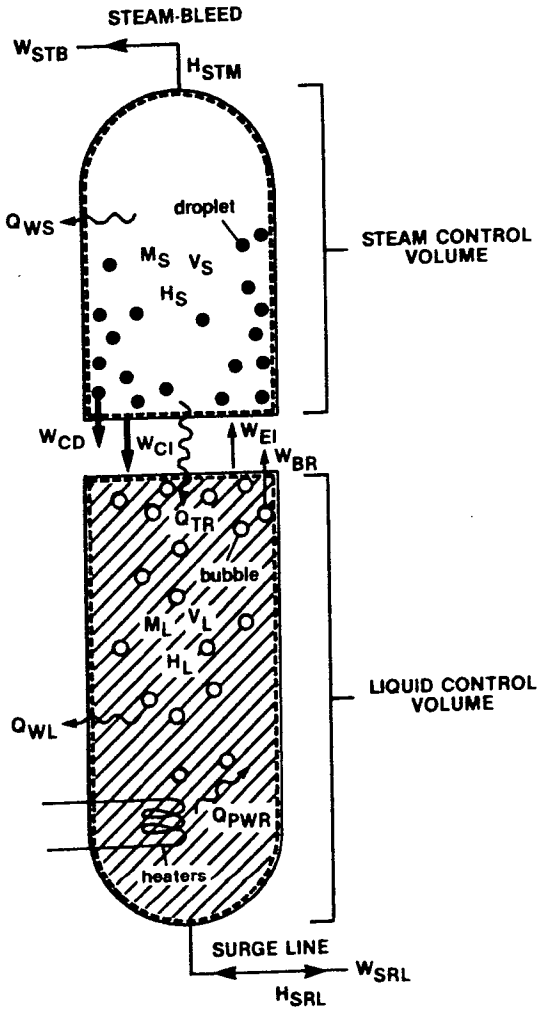

FIGURE 2.

Schematic of pressurizer control volumes

When there is a need to obtain detailed profiles of flow parameters in any one or more of the control volumes, the lumped formulation on the control volume(s) can be replaced by sets of one-dimensional drift-flux model formulations. The drift-flux formulation consists of five differential equations: mixture continuity, mixture momentum, mixture energy, dispersed phase continuity and equation of state (See Equation A6 to A9 and A12, A13 in Appendix A).

When the drift-flux formulation is used, values of local drift-flux parameters are integrated over the control volume and their volume-averaged values are determined. The purpose of obtaining these averaged values is two-fold. First, averaging ensures that the drift-flux formulation is compatible with the rest of the IDRIFF models' structure, which is based on the lumped formulation. Second, the averaged values are used to set up boundary conditions for neighboring control volumes.

The swell and shrink of the control volume are calculated based on the results of the lumped model (mass inventory and movement of interface due to pressure difference between the liquid control volume and the steam control volume) and the integrated results of the drift-flux model (void fraction). The approach of using the drift-flux concept to calculate liquid level in a lumped pressure vessel model is similar to that by Wulff et al. [10], except that, in the latter, the expression estimating the liquid level is analytically derived from the drift-flux concept. In the present work, however, the drift-flux differential equations are solved locally at each grid-point and the results are numerically integrated.

In addition, a simplified momentum equation is implemented in the lumped calculation. Due to the nature of the pressurizer, where the liquid is basically stagnant, the momentum equation is used to calculate only the vertical movement of the liquid surface due to pressure difference between the steam control volume and the liquid control volume, as mentioned previously.

Furthermore, the following are implemented as parts of the lumped formulation component of the code: bubble rise submodel, droplet drop submodel, interface evaporation and condensation submodel, steam-bleed flow submodel, surge-line flow submodel, heat generation from electrical heaters and calculations of heat distribution due to heat evaporation and condensation.

The steam control volume and the liquid control volume are assumed to be at each of their own saturation condition under their respective average pressures. Hence, the thermodynamic properties of the steam control volume and the liquid control volume are functions of their respective average pressures and qualities.

The simulations of the transient experiments consist of two parts: the preparation of the initial quasi-steady-state and the actual transient. Both parts are simulated by using the transient calculation of the IDRIFF code. In the first part, the values of steam pressure, liquid pressure (with correction due to any hydrostatic pressure difference), liquid temperature and liquid level of the initial 'cold' pressurizer condition measured in the experiment are input as initial conditions. Values of heater power, ambient

temperature and atmospheric pressure measured from the experiment are used as boundary conditions.

In addition, various values of the steam bleed valve opening are tried, such that the predicted steam-bleed flow is approximately equal to the average of that measured in the experiment. The simulation is carried out until the corresponding quasi-steady-state is reached. The calculated condition of the pressurizer becomes the initial condition of the actual transient simulation.

The simulation of the actual transient is more straight-forward. Boundary conditions according to that measured in the experiment are imposed on the calculation. The simulation is carried out until another quasi-steady-state is reached. Specifically, the method of applying the boundary conditions depends on the types of the transients as follows:

(a) Step-change in heater power: The electrical power to the heaters, Q_{PWR}, recorded in the experiment is inputted. The heater submodel in the code calculates values of the transient of heat input to the fluid, Q_{HEATR}, which in turn becomes the boundary condition to the numerical calculation. Steam-bleed valve opening, surge-line flow (zero flow) and other environmental conditions are maintained at their initial condition values.

(b) Step-change in the steam-bleed valve opening: The steam-bleed valve opening used for the boundary condition to the calculation is varied so that the calculated steam-bleed flow changes at approximately the same rate and peaks at approximately the same values as those measured in the experiment. Heater power, surge-line flow (zero flow) and other environmental conditions are maintained at their initial condition values.

(c) Perturbation of the surge flow: the experimentally measured surge flow and temperature of the fluid in the surge line (in case of insurge) are directly used as boundary conditions. Values of steam-bleed valve opening, heater power and other environmental conditions are maintained at their initial condition values.

4. TRANSIENT WITH STEP CHANGE IN HEATER POWER

An example of transients following a step-wise increase in the pressurizer heater power is reported in this section, followed by a discussion on an example of transient following a step-wise decrease in the heater power.

The pressurizer is initially at a quasi-steady-state under a saturation pressure of 144 kPa(a). The heater's power is maintained at 335.5 watts. The steam-bleed valve is relieving steam at approximately constant rate of 1.3×10^{-4} kg/s. The liquid level is at 23 cm. Bubbly flow pattern is observed in the liquid volume.

At the time of perturbation, which is about 17 s after measurement was initiated, heater power was increased rapidly to 680 watts.

The transient response of two-phase parameters measured in the experiment are

plotted in Figures 3 to 7: steam pressure (P_{SA}) in Figure 3; liquid temperature (T_{LA}) in Figure 4; void fraction in the liquid volume (α_{gL}) in Figure 5; and steam-bleed flow (W_{STB}) in Figure 6. The liquid levels, which were determined from photographs, are plotted in Figure 7.

Starting from a simulated quasi-steady-state condition correspondent to that in the experiment, the transient of the pressurizer following the heater power step-up perturbation is simulated by applying the measured electrical power to the IDRIFF code as a boundary condition. The transient of average steam pressure predicted by the IDRIFF code is commpared with the experimentally measured steam pressure and is shown in Figure 3. Similarly, predicted transients of average liquid temperature, average void fraction in the liquid volume, steam-bleed flow and liquid level are plotted in Figures 4 to 7, respectively, and to be compared with their corresponding experimentally measured values.

It can be observed that following a step-increase in heater power, the void fraction in the liquid volume tends to increase, but is limited by the steam-bleed flow. The steam-bleed flow will eventually increase following the increase in pressure. The void fraction hence will eventually increase to a value corresponding to the new setting of heater power and steam-bleed flow.

The sudden increase of the experimentally measured void fraction after about 400 s may be caused by the transition of flow-regime. This in turn causes an accumulation of vapour in the steam volume and subsequent bursting of steam from the steam bleed valve at about 510 s. The change in flow regime was not done automatically in the current version of the IDRIFF code.

A typical example of transients where the heater power is suddenly decreased step-wise is discussed in the following.

The initial quasi-steady-state of the pressurizer is under a saturated pressure of 144.5 kpa(a). The heater power is set at 326 watt. The steam-bleed flow is fluctuating at a value of 0.143×10^{-3} kg/s. The liquid level is at about 23 cm. Bubbly flow is observed in the liquid volume. At about 28 s after measurement began to be taken, the heater power is step-wisely decreased to 182 watts.

Both the experiment and the IDRIFF simulation indicate that following the step-wise decrease in heater power, void fraction, liquid level, liquid and steam pressure and temperature decrease gradually as one expected. The transient of the steam pressure is shown in Figure 8.

The IDRIFF code also provides additional information that may not be directly observed in the experiment. For example, the transient of the heat transfer rate from the liquid volume to the steam volume predicted by the IDRIFF is shown in Figure 9. It indicates that the steam temperature decreases at a rate relatively faster than that of the liquid. This is confirmed on the experimental measurements and the code's prediction of the temperatures. This can be explained by the following. The liquid volume is initially at a saturation condition while the steam volume is initially at slightly superheated condition. The steam pressure is less than the liquid pressure due to the hydrostatic pressure difference. Steam temperature, on the other

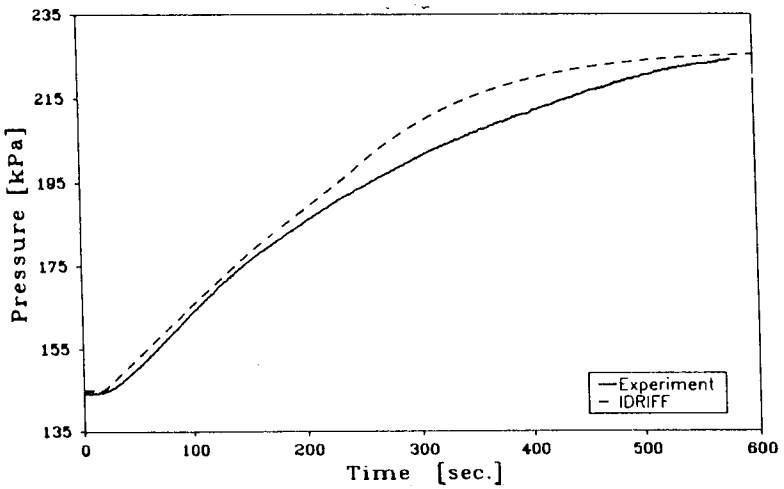

FIGURE 3. Case 1 - Step Increase of Heater Power: Transient of average pressure in the steam control volume

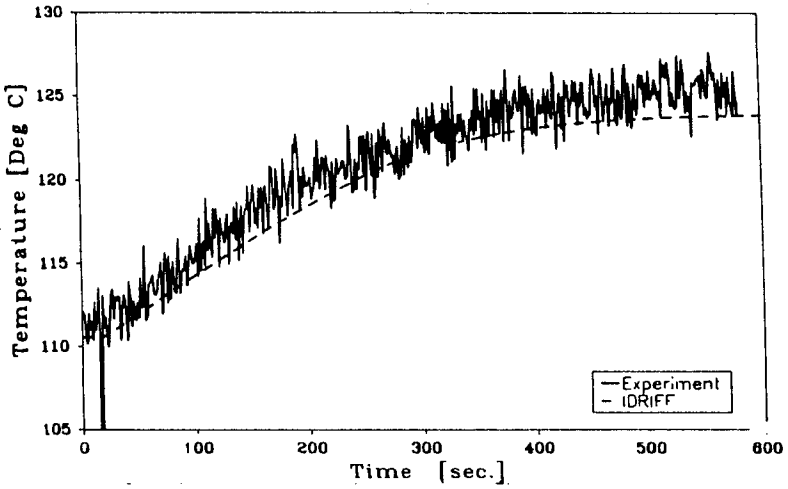

FIGURE 4. Case 1 - Step Increase of Heater Power: Transient of average liquid temperature in the liquid control volume

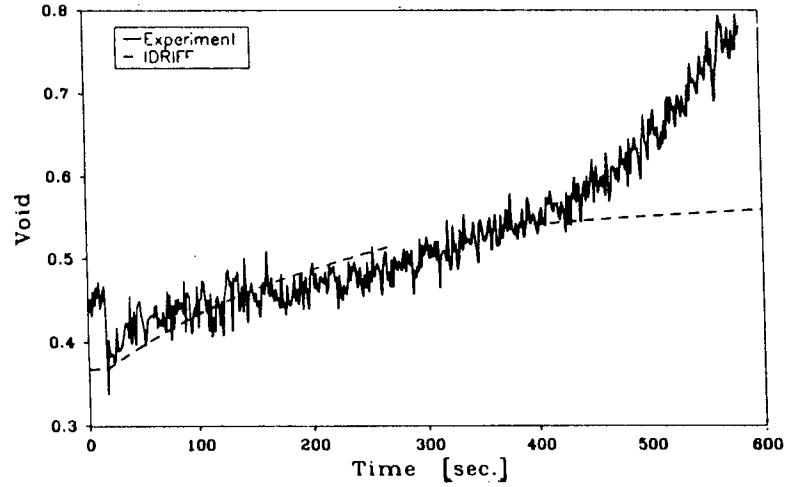

FIGURE 5. Case 1 - Step Increase of Heater Power: Transient of average void fraction in the liquid control volume

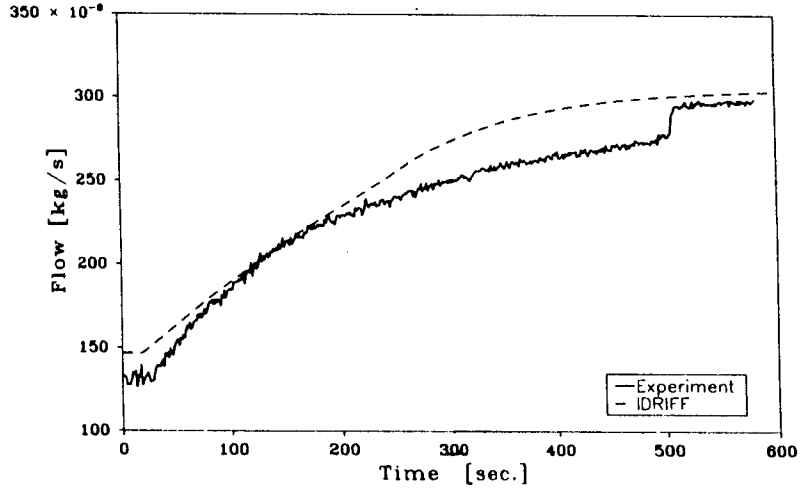

FIGURE 6. Case 1 - Step Increase of Heater Power: Transient of steam-bleed flow

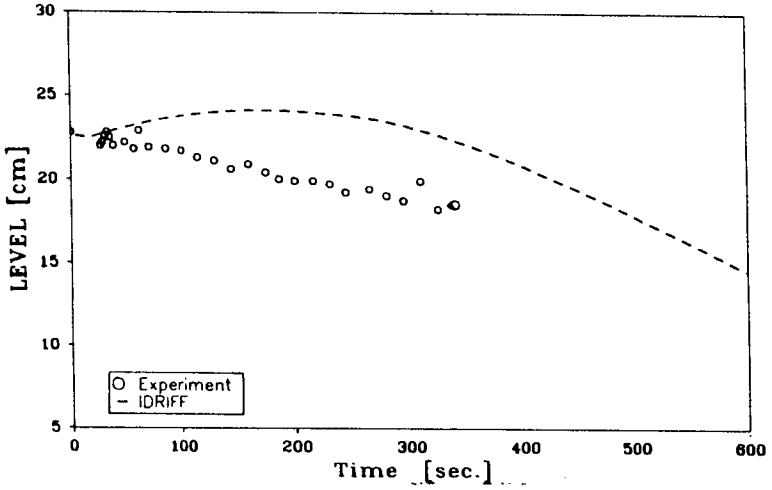

FIGURE 7. Case 1 - Step Increase of Heater Power: Transient of liquid level

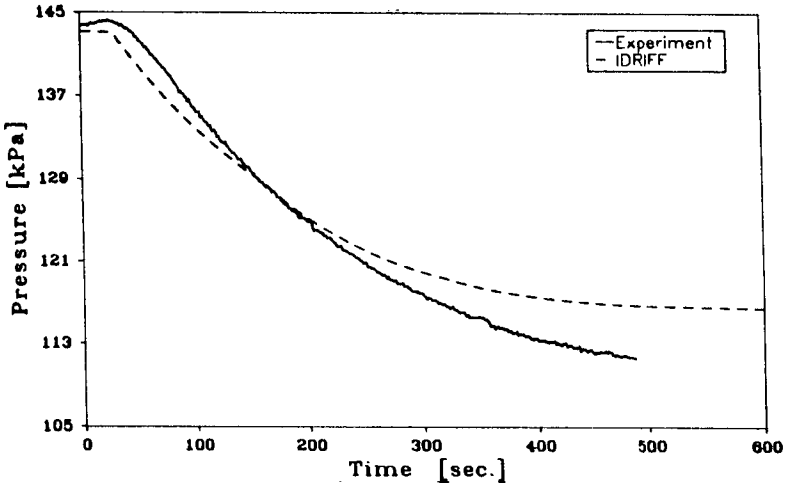

FIGURE 8. Case 2 - Step Decrease of Heater Power: Transient of average pressure in the steam control volume

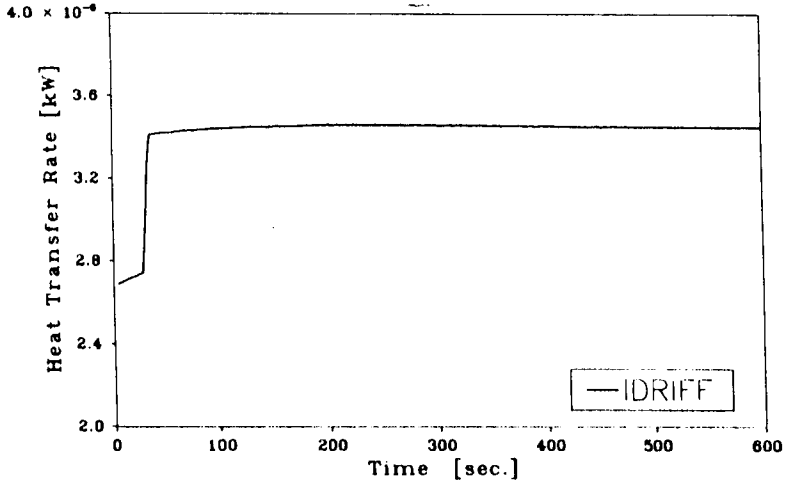

FIGURE 9. Case 2 - Step Decrease of Heater Power: Transient of heat transfer rate from liquid control volume to steam control volume

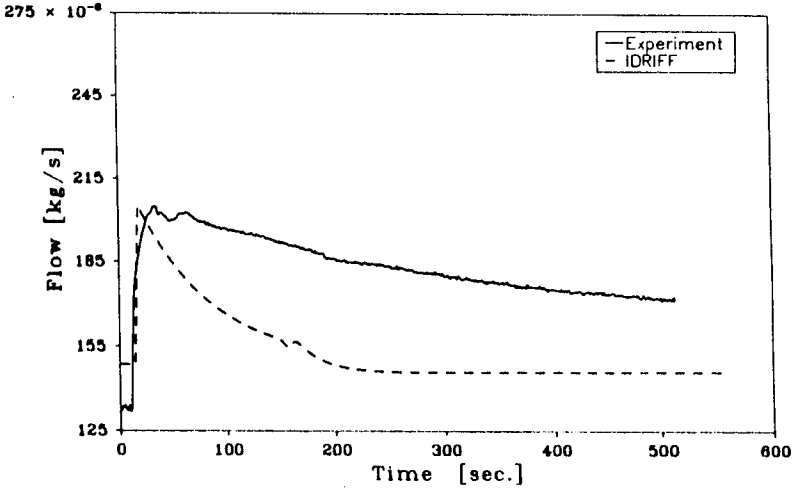

FIGURE 10. Case 3 - Step Increase of Steam-bleed valve opening: Transient of steam-bleed flow

hand, is maintained at above its saturation temperature by the continuous supply of vapour from the liquid volume, which has a slightly higher saturation temperature. When the heater power is suddenly reduced, the quality in the liquid volume decreases drastically; however, its saturation is basically maintained. Hence the liquid temperature drop is mainly due to the decrease of saturation temperature as liquid pressure decreases. On the other hand, different phenomena is likely to happen in the steam volume. Although pressure decrease in the steam volume due to decreases of both net mass and energy influx to the steam volume, the temperature drops at a faster rate since the supply of vapour that is used to maintain its superheated temperature level is now reduced. In general, the steam volume will return to saturation condition or sometimes subcooled condition, with its temperature decreaseing at a faster rate than its saturation temperature.

5. TRANSIENT WITH STEP-CHANGE IN STEAM-BLEED VALVE OPENING

An example of the transient with step-wise increase in steam-bleed valve opening is first discussed in this section.

Initially, the pressurizer is at a quasi-steady-state under a saturation pressure of 159.5 kpa(a). The heater power is at 335.5 watt. The liquid level is at 2.5 cm. Bubbly flow is observed in the liquid volume.

The steam-bleed valve opening is set at this initial condition such that the steam bleed flow is measured to be about 1.47×10^{-3} kg/s. At about 15 s after the experimental measurements begin to be taken, the steam-bleed valve opening is suddenly increased. The transient of the steam-bleed flow measured in the experiment is shown in Figure 10. The discrepancy between the measured steam-bleed flow and that predicted by the IDRIFF code in Figure 10 was caused by both the inadequacy of the steam-bleed model in the code as well as the inaccuracy of the steam-bleed flow when two phase mixture was bled through the steam-bleed valve.

The transient of the major parameters: steam pressure, liquid temperature, void fraction in the liquid volume and liquid level, both measured and predicted by the IDRIFF code, are shown in Figure 11 to 14 respectively.

Examples of additional parameters predicted by the IDRIFF code are the rate of interface evaporation shown in Figure 15 and the rate of condensate drop dropping shown in Figure 16.

Basically, the sudden increase of the steam-bleed flow after the valve opening is increased causes rapid depressurization of the pressurizer. There is a sudden increase of the gas phase leaving the liquid volume as shown in Figure 15. The drastic increase in the movement of the gas phase causes the void fraction in the liquid volume to surge as shown in Figure 13. But the increase in the amount of gas phase leaving the liquid volume is short-lived since the generation of the vapour is limited as the heater power remains constant. As the steam volume is losing its mass, steam pressure and hence pressure at other locations as well continue to drop. The decrease of the steam pressure reduce the amount of steam being relieved through the steam-bleed valve. The steam-bleed flow gradually decreases to its initial value.

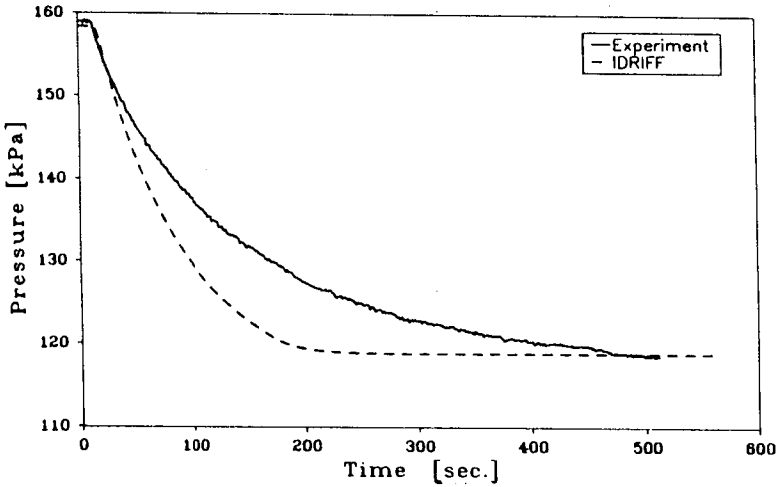

FIGURE 11. Case 3 - Step Increase of Steam-bleed valve opening: Transient of average pressure in steam control volume

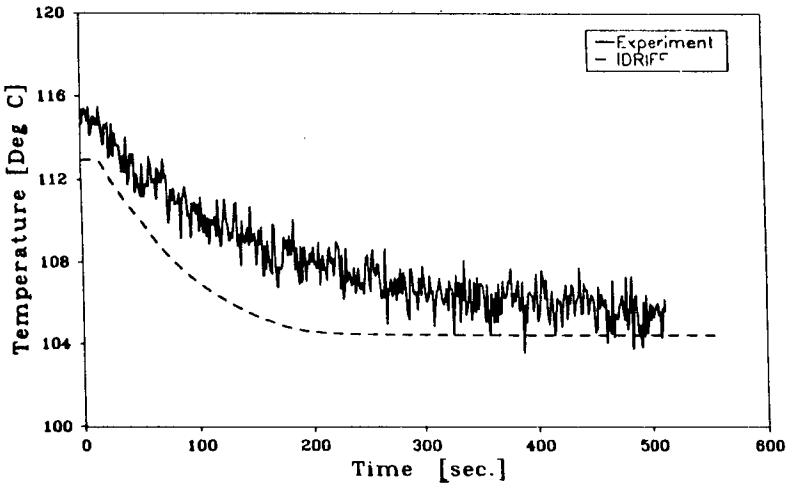

FIGURE 12. Case 3 - Step Increase of Steam-bleed valve opening: Transient of average temperature in liquid control volume

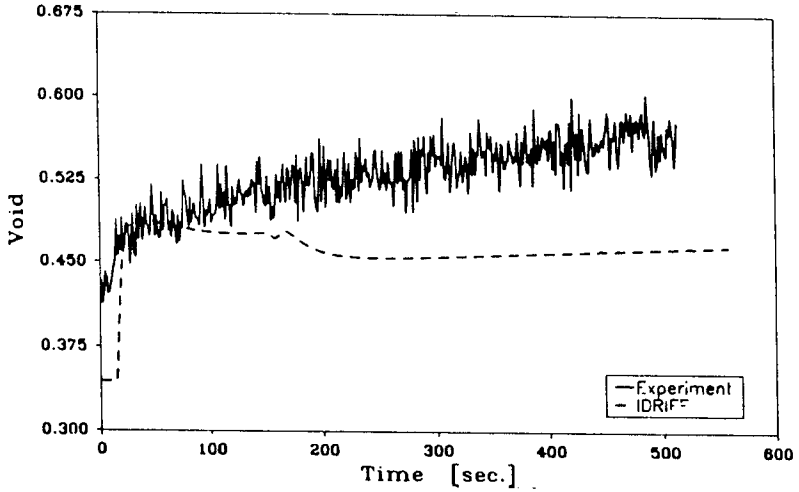

FIGURE 13. Case 3 - Step Increase of Steam-bleed valve opening: Transient of void fraction in liquid control volume

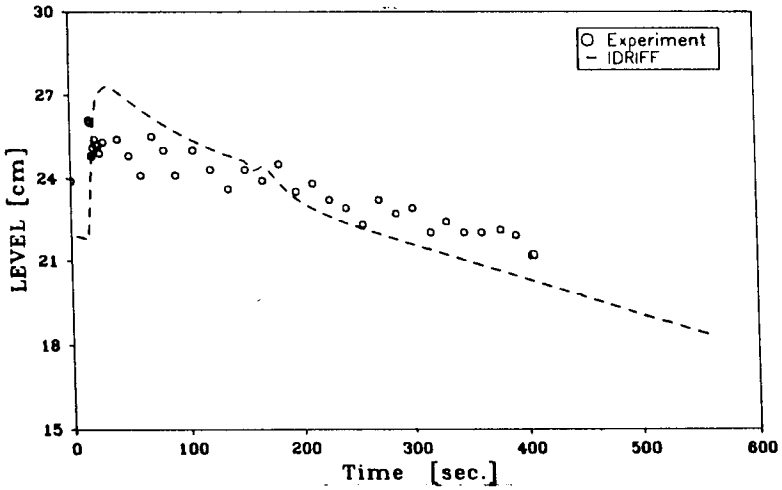

FIGURE 14. Case 3 - Step Increase of Steam-bleed valve opening: Transient of liquid level

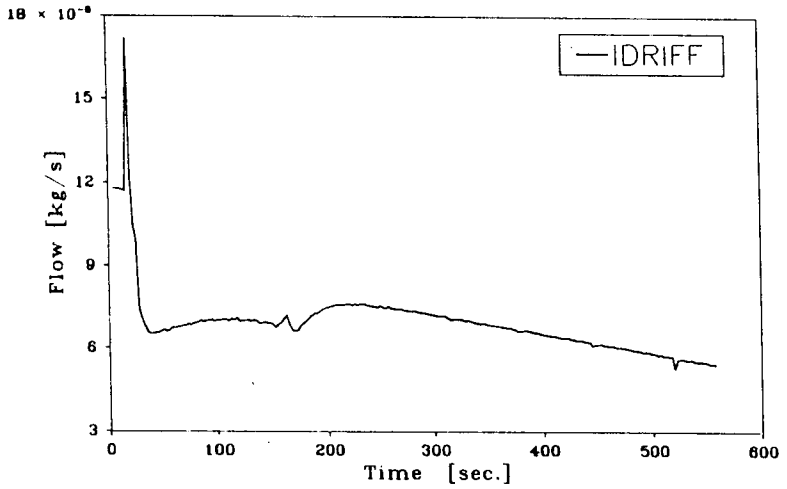

FIGURE 15. Case 3 - Step Increase of Steam-bleed valve opening: Transient of interface evaporation rate

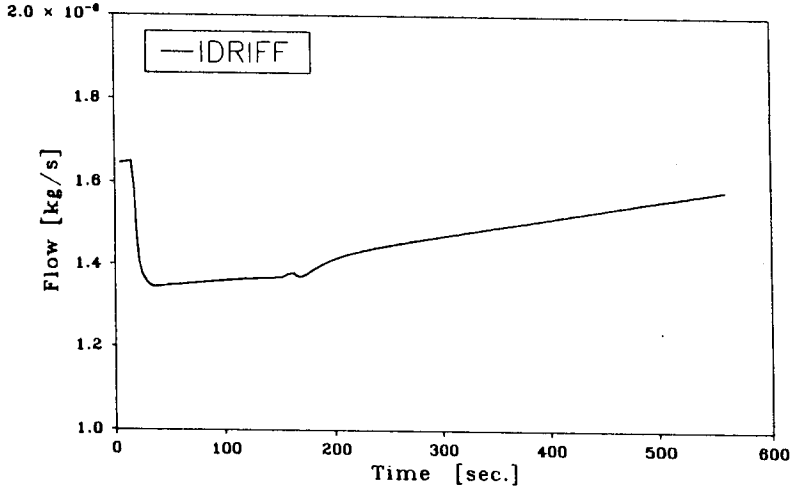

FIGURE 16. Case 3 - Step Increase of Steam-bleed valve opening: Transient of condensate drops droping rate

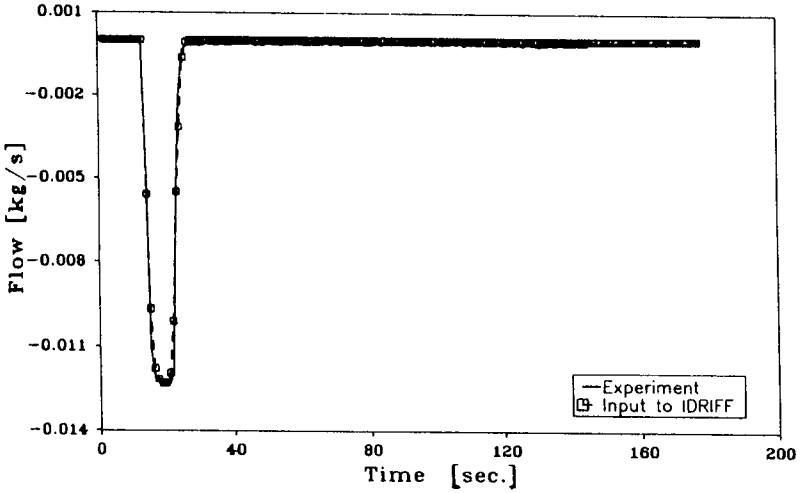

FIGURE 17. Case 5 - Sudden and Short-lived Outsurge: Transient of surge-line flow

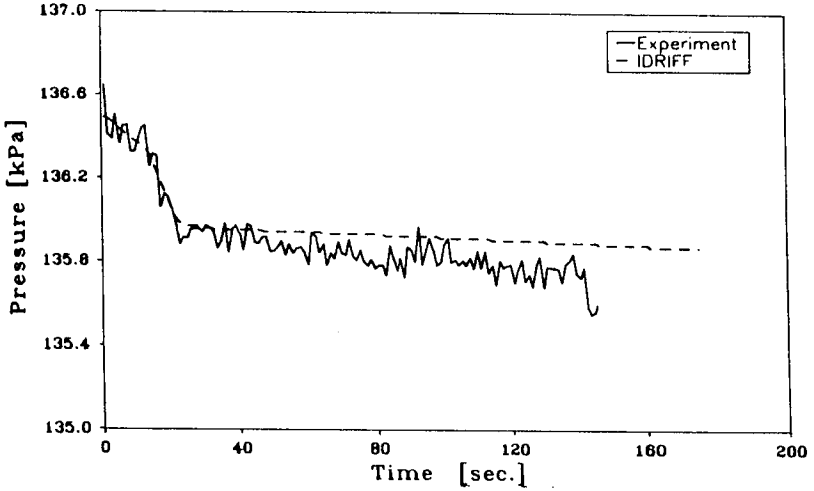

FIGURE 18. Case 5 - Sudden and Short-lived Outsurge: Transient of average pressure in steam control volume

Similar to the observation in the previous case in Section 5, the temperature in the steam volume is basically controlled by the supply of vapour from the liquid volume, which is saturated under a saturation pressure slightly higher than the steam pressure. As supply of the gas phase to the steam volume is reduced drastically, the temperature in the steam volume decreases at a rate faster than its saturation temperature, which decreases with the steam pressure. As a result, condensation takes place, as indicated in Figure 16.

There was not much surprise in the study of the transient following a sudden decrease of steam-bleed valve opening. Basically, as the movement of the gas phase is more restricted, the void fraction in the liquid volume initially decreases. However, as heater power remains constant, reducing the steam-bleed flow will only cause the system pressure to rise. The increase in pressure will eventually drive the steam-bleed flow up and close to its initial value. The value of the void fraction will also eventually increase.

6. TRANSIENT WITH SUDDEN AND SHORT-LIVED OUTSURGE AND INSURGE

In the four transient cases described in the previous two sections, the pressurizer is isolated from the simulated PHT system in the experiment by closing the surge-line valve. In the simulation, this was simulated by applying zero surge flow as a boundary condition to the pressurizer in the IDRIFF code's calculation. In this section, the effect of the surge flow will be investigated. First, an example of the transient with short-lived, pulse-wise outsurge is now discussed.

Initially, the pressurizer is at quasi-steady-state under a saturation pressure of 137 kPa(a). The heater is maintained at 261 watts. The steam-bleed valve opening is set such that the steam-bleed flow is approximately 1.14×10^{-4} kg/s. The surge line valve is closed. The liquid level is at 26.5 cm. Bubbly flow pattern is observed in the liquid volume.

The simulated PHT system is maintained at about 105 kPa(a) and is at saturation. At about 12 s after the measurements are taken in the experiment, the surge-line valve is opened suddenly and is closed about 8.5 seconds later. The flow of the fluid from the pressurizer, through the surge-line into the simulated PHT system is shown in Figure 17. This transient of the surge flow is digitized and is input as a boundary condition in the simulation of the transient.

The comparisons of the experimental measured steam pressure, liquid temperature, the void fraction in the liquid volume, and the liquid level, with their corresponding values predicted by IDRIFF are plotted in Figures 18 to 21.

When the surge line valve was opened, fluid in the bottom part of the pressurizer flows out of the pressurizer, causing the liquid inventory and hence the liquid level to drop abruptly. The remaining fluid in the pressurizer sees an expansion of volume per unit mass. As a result, the system pressure decreases, but at an almost insignificant rate. The decrease in fluid density also caused the temperature to drop somewhat. However, the decrease is less than the noise in the measurements. The sudden expansion of

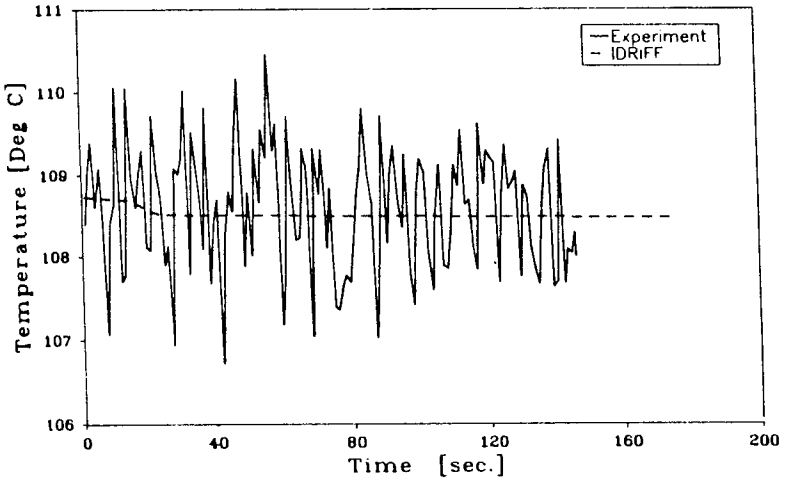

FIGURE 19. Case 5 - Sudden and Short-lived Outsurge: Transient of average temperature in liquid control volume

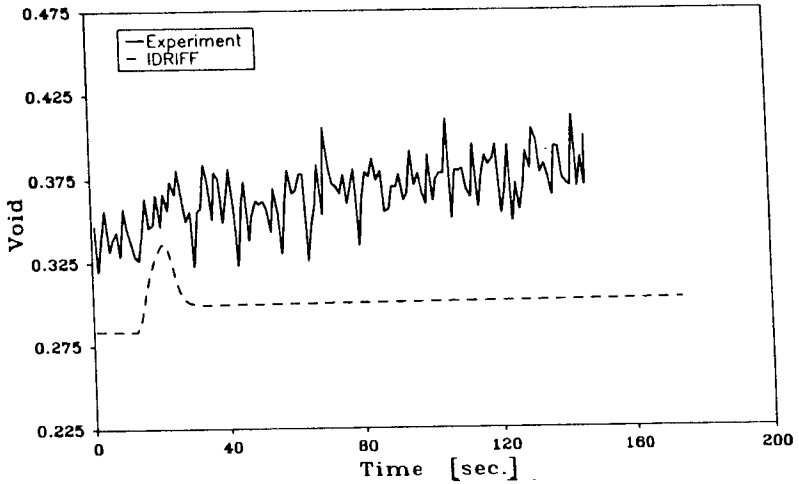

FIGURE 20. Case 5 - Sudden and Short-lived Outsurge: Transient of void fraction in liquid control volume

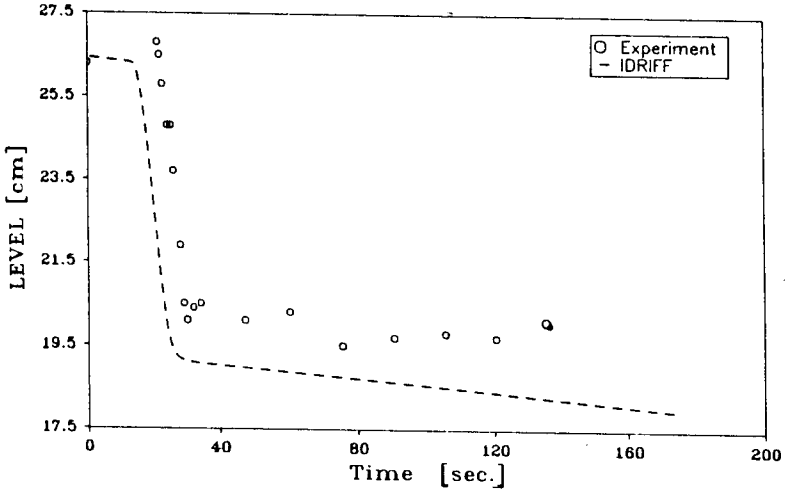

FIGURE 21. Case 5 - Sudden and Short-lived Outsurge: Transient of liquid level

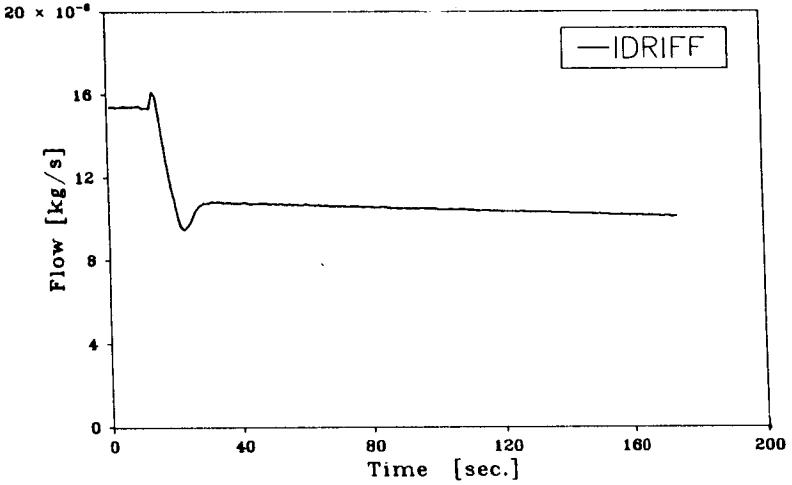

FIGURE 22. Case 5 - Sudden and Short-lived Outsurge: Transient of interface evaporation rate

the volume (per unit mass) of the fluid causes the quality to surge and then drop back as the system approaches a new equilibrium. This can be indicated by the transient of the void in the liquid volume in Figure 21.

An interesting phenomena that occurs in this transient is the condensation in the steam volume. It is apparent from the decrease of the interfacial evaporation rate (Figure 22) that the liquid pressure decreases at a rate faster than that of the steam pressure. However, the temperature in the steam volume depends on the temperature of vapour, which is supplied from the liquid volume; since the liquid volume is basically at saturation, the steam temperature therefore decreases together with the saturation temperature of the liquid volume. As a result, the temperature in the steam volume decreases faster than the saturation temperature in the steam volume, causing condensation to take place. The condensation is evident in the plot of the droplet dropping rate in Figure 23.

An example of the transient, with a short duration of pulse insurge, will now be discussed.

Initially, the pressurizer is at a quasi-steady-state under a saturation pressure of 134.8 kPa(a). The heater is at 266.4 watt. The steam-bleed flow is 1.15×10^{-4} kg/s and the surge flow is kept at zero by closing the surge-line valve. The liquid level is at about 19.6 cm. Bubbly flow is observed in the liquid volume.

The simulated PHT system is maintained at about 170 kPa(a) and a subcooled temperature of about 85 C. At about 6 s after the measurements are taken in the experiment, the surge-line valve is opened suddenly and is closed 6.5 s later. The recorded insurge flow is shown in Figure 24. This transient of the insurge flow is used directly as a boundary condition to pressurizer in the simulation.

Generally, when the insurge fluid enters the pressurizer, the total mass in the liquid volume and hence the liquid level increase rapidly (Figure 25), compressing the steam volume. Since the incoming fluid is subcooled and at a temperature lower than that of the fluid initially in the pressurizer, the immediate consequence is the rapid dropping of the quality and hence the void in the liquid volume, as shown in Figure 26. Meanwhile, as energy per unit mass in the liquid volume also decreases, the pressure and temperature in the liquid volume also decreases. As a result of decrease of quality in the liquid volume, the amount of the gas phase leaving the liquid volume into the steam volume becomes limited. This in turn results in the decrease of steam pressure (Figure 27) and temperature. Subsequently, the steam-bleed flow decreases as well. However, during this time, the heater power remains constant, the continued supply of heat from the heater eventually restores the energy content of the pressurizer. As a result, the pressure, temperature, and void fraction gradually return to their initial values, respectively.

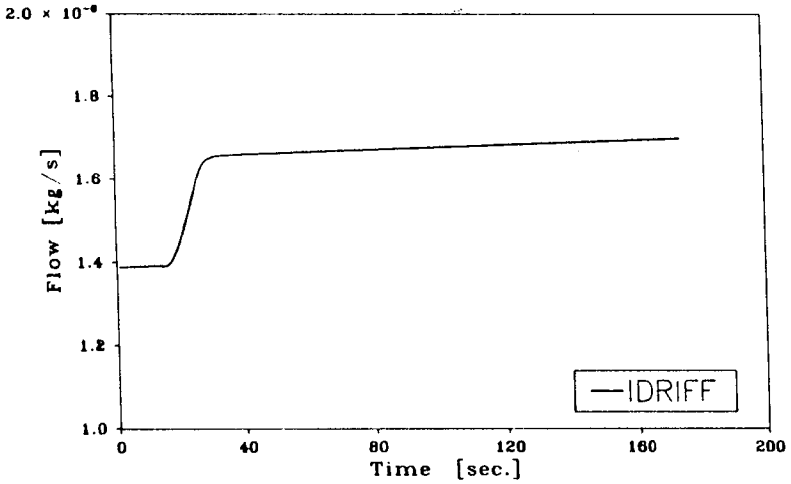

FIGURE 23. Case 5 - Sudden and Short-lived Outsurge: Transient of condensate drops droping rate

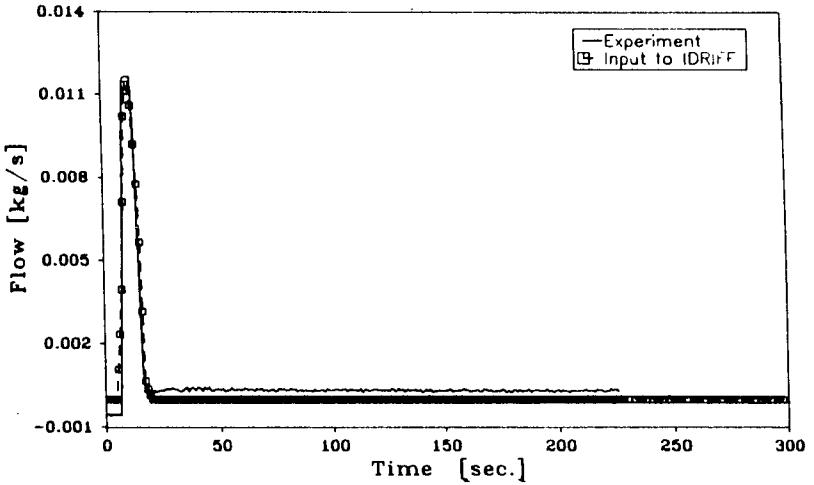

FIGURE 24. Case 6 - Sudden and Short-lived Insurge: Transient of surge-line flow

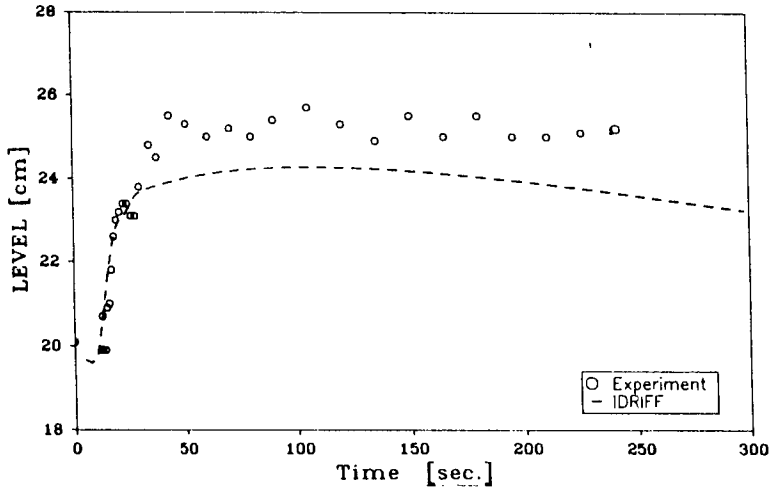

FIGURE 25. Case 6 - Sudden and Short-lived Insurge: Transient of liquid level

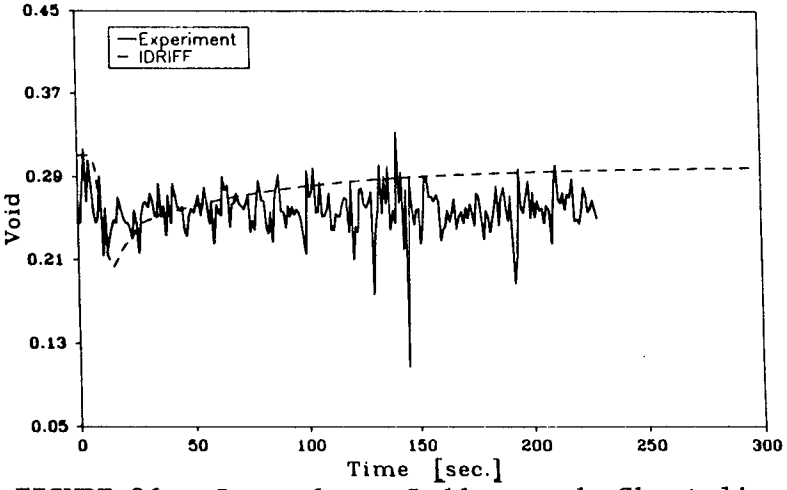

FIGURE 26. Case 6 - Sudden and Short-lived Insurge: Transient of void fraction in the liquid control volume

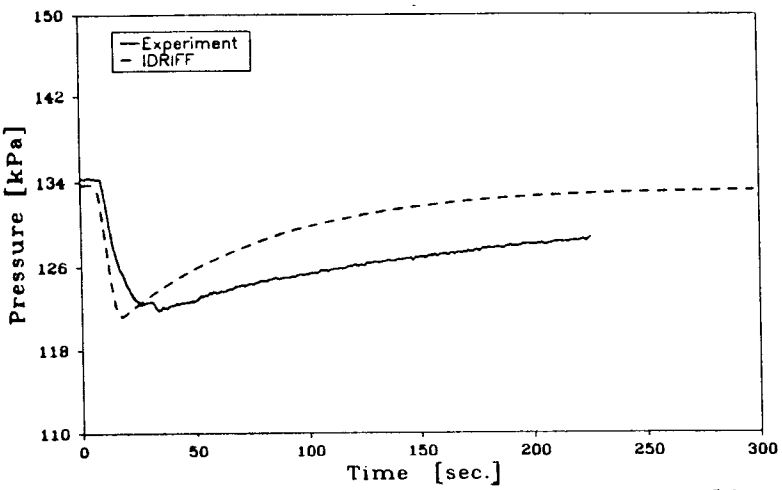

FIGURE 27. Case 6 - Sudden and Short-lived Insurge: Transient of average pressure in the steam control volume

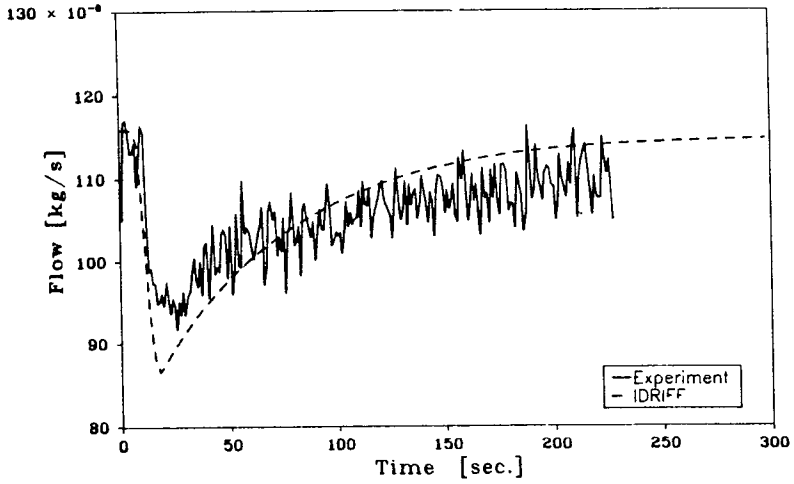

FIGURE 28. Case 6 - Sudden and Short-lived Insurge: Transient of steam-bleed flow

7. CONCLUSIONS

Based on the results obtained in the current study, some of which have been presented in Sections 4, 5 and 6, the following can be concluded:

1) The IDRIFF code predicts the transient behaviour of all pressurizer parameters with reasonably good agreement qualitatively. Moreover, quantitative discrepancies between values of pressure and temperature calculated by IDRIFF and those experimentally measured are within 8% during the transient. The discrepancy for the liquid level varies between 0 to 20% during the transient.

2) The IDRIFF code predicts the values of all pressurizer parameters, except for void fraction, at the final quasi-steady-state conditions within 3% accuracy. The discrepancy for the void fraction is less than 29%.

3) When the control parameters (heater power and steam-bleed flow) of an isolated pressurizer initially at quasi-steady-state is perturbed, the pressurizer will adjust itself and eventually reach another quasi-steady-state. At which time, all parameters will approach their new equilibrium values. At the beginning of the transient immediately following the perturbation, the following behaviours are generally observed:

   i) the pressure and temperature of both gas-phase and liquid-phase, the void fraction in the liquid-volume, the liquid level and the steam-bleed flow increase with heater power, and
   ii) the pressure and temperature of both gas-phase and liquid-phase decrease with the steam-bleed flow, however, the void fraction in the liquid-volume and the liquid level increase with the steam-bleed flow.

4) When a pressurizer initially at a quasi-steady-state is subjected to a pulsed type of outsurge or insurge, the effect is basically a depressurization process or a pressurization process in the pressurizer, respectively. In addition, during an insurge, if the incoming fluid has a different energy per unit mass (or roughly different temperature) than that originally in the pressurizer, the transient will be complicated by a process of energy redistribution within the pressurizer.

5) The void fraction in the liquid volume of a pressurizer is controlled by both the heater power and the steam-bleed flow. If only one of the two control parameters is changed, the resulting change in the void fraction is constrained by the value of the other control parameters as well.

6) The temperature in the steam volume of a pressurizer is mainly determined by the temperature of the vapour leaving (or evaporating from) the liquid volume and hence by the temperature of the gas-phase in the liquid volume; the liquid volume is generally closer to saturation at a quasi-steady-state, while the steam volume may further depart from a saturational equilibrium (superheated or rapid condensation).

Finally, the current investigation of single-parameters perturbation-type of transient in the pressurizer has provided many useful insights on the behaviour of the pressurizer. These can be used as a basis for further study on general transients of the pressurizer, where more than one perturbation is usually found.

APPENDIX A

Summary of IDRIFF Code Mathematical Models

Lumped Formulation

$$\frac{dM_L}{dt} = W_{SRL} - W_{EI} - W_{BR} + W_{CD} + W_{CI}, \tag{A1}$$

$$\frac{dM_S}{dt} = -W_{STB} - W_{CD} - W_{CI} + W_{EI} + W_{BR} \tag{A2}$$

$$\frac{dH_L}{dt} = -(W_{SRL} \cdot h_{SRL}) - (W_{EI} \cdot h_{fLQ}) - (W_{BR} \cdot h_{gLQ}) + (W_{CI} \cdot h_{fST})$$
$$+ (W_{CD} \cdot h_{fST}) - Q_{WL} + Q_{HEATR} - Q_{TR} - \beta[(1-\delta)Q_{COND} + Q_{EVPR}], \tag{A3}$$

$$\frac{dH_S}{dt} = -(W_{STB} \cdot h_{gST}) - (W_{CD} \cdot h_{fST}) - (W_{CI} \cdot h_{gST}) + (W_{EI} \cdot h_{gLQ})$$
$$+ (W_{BR} \cdot h_{gLQ}) - Q_{WS} + Q_{TR} - (1-\beta)[(1-\delta)Q_{COND} + Q_{EVPR}] \tag{A4}$$

$$\frac{dV_S}{dt} = -\frac{dV_L}{dt} \tag{A5}$$

Drift-Flux Formulation

Mixture continuity equation:

$$\frac{\partial <\rho_m>}{\partial t} + \frac{\partial}{\partial z}(<\rho_m> \bar{v}_m) = 0 \tag{A6}$$

Continuity equation for the dispersed phase:

$$\frac{\partial <\alpha_d> \rho_d}{\partial t} + \frac{\partial}{\partial z}(<\alpha_d> \rho_d \bar{v}_m) = <\Gamma_d> - \frac{\partial}{\partial z}\left(\frac{<\alpha_d> \rho_d \rho_c}{<\rho_m>} v_{dj}\right) \tag{A7}$$

Mixture momentum equation:

$$\frac{\partial <\rho_m> \bar{v}_m}{\partial t} + \frac{\partial}{\partial z}(<\rho_m> \bar{v}_m^2) = \frac{\partial}{\partial z}<P_m> + \frac{\partial}{\partial z}<\tau_{zz} + \tau_{zz}^T>$$

$$- <\rho_m> g_z - \frac{f_m}{2D} <\rho_m> \bar{v}_m |\bar{v}_m| - \frac{\partial}{\partial z}\left[\frac{<\alpha_d> \rho_d \rho_c}{(1 - <\alpha_d>) <\rho_m>} v_{dj}^2\right] \qquad (A8)$$

$$- \frac{\partial}{\partial z} \sum_k \mathrm{COV}(\alpha_k \rho_k v_k v_k) + <M_m>;$$

Mixture enthalpy energy equation:

$$\frac{\partial <\rho_m> \bar{h}_m}{\partial t} + \frac{\partial}{\partial z}(<\rho_m> \bar{h}_m \bar{v}_m) = -\frac{\partial}{\partial z} <q + q^T> + \frac{\dot{q}_w'' \xi_h}{A}$$

$$- \frac{\partial}{\partial z}\left[\frac{<\alpha_d> \rho_d \rho_c}{<\rho_m>} \Delta h_{dc} v_{dj}\right] - \frac{\partial}{\partial z} \sum_k \mathrm{COV}(\alpha_k \rho_k h_k v_k) + \qquad (A9)$$

$$+ \frac{\partial}{\partial z} <P_m> + \left[\bar{v}_m + \frac{<\alpha_d> \rho_d \rho_c}{<\rho_m>} v_{dj}\right] \frac{\partial <P_m>}{\partial z} + <\Phi_m^{\mu}> + <\Phi_m^{\sigma}> + <\Phi_m^{i}>$$

Equation of State

$$\frac{\partial P_{LA}}{\partial t} = G_1(P_{LA}, x_L) \frac{\partial h_L}{\partial t} + G_2(P_{LA}, x_L) \frac{\partial \rho_L}{\partial t}. \qquad (A10)$$

$$\frac{\partial P_{SA}}{\partial t} = G_1(P_{SA}, x_S) \frac{\partial h_S}{\partial t} + G_2(P_{SA}, x_S) \frac{\partial \rho_S}{\partial t} \qquad (A11)$$

$$\frac{\partial <P_m>}{\partial t} = G_1(P_m, x_m) \frac{\partial \bar{h}_m}{\partial t} + G_2(P_m, x_m) \frac{\partial <\rho_m>}{\partial t} \qquad (A12)$$

$$\frac{\partial P_d}{\partial t} = G_1(P_m, x_m) \frac{\partial \bar{h}_m}{\partial t} + G_2(P_m, x_m) \frac{\partial <\rho_m>}{\partial t} - \Delta P \frac{\partial <\alpha_d>}{\partial t} \qquad (A13)$$

The coefficient functions G_1 and G_2 are defined as:

$$G_1(P,x) = \frac{v_g - v_f}{\left[x \frac{dh_g}{dP} + (1-x)\frac{dh_f}{dP}\right](v_g - v_f) - \left[x \frac{dv_g}{dP} + (1-x)\frac{dv_f}{dP}\right](h_g - h_f)} \qquad (A14)$$

and

$$G_2(P,x) = \frac{(h_g - h_f)/\rho^2}{\left[x\frac{dh_g}{dP} + (1-x)\frac{dh_f}{dP}\right](v_g - v_f) - \left[x\frac{dv_g}{dP} + (1-x)\frac{dv_f}{dP}\right](h_g - h_f)} \qquad \text{(A15)}$$

Nomenclature

(The letters 'L' or 'D' within parentheses at the end of some definition indicates whether the parameter defined is specifically used in the Lumped calculation or in the Drift-Flux calculation.)

A Pressurizer cross-sectional area

D Pressurizer cross-sectional diameter

f_m Two-phase flow friction coefficient (D)

G_1, G_2 Coefficient functions in the rate form of equation of state

g Acceleration due to gravity

g_z Component of the gravitational acceleration in the axial direction (D)

h_f Saturated liquid phase specific enthalpy

h_{fLQ} Average saturated liquid-phase specific enthalpy in the liquid control volume (L)

h_{fST} Average saturated liquid-phase specific enthalpy in the steam control volume (L)

h_g Saturated gas-phase specific enthalpy

h_{gLQ} Average saturated gas-phase specific enthalpy in the liquid control volume (L)

h_{gST} Average saturated gas-phase specific enthalpy in the steam control volume (L)

h_S Average specific enthalpy of mixture in the steam control volume (L)

h_L Average specific enthalpy of mixture in the liquid control volume (L)

h_c Local continum phase specific enthalpy (D)

h_d Local dispersed phase specific enthalpy (D)

h_m Local mixture specific enthalpy (D)

h_{SRL} Specific enthalpy of the fluid in the surge line (L)

M_L Total mass of mixture in the steam control volume (L)

M_m Local interfacial momentum source (D)

M_S Total mass of mixture in the steam control volume (L)

P Pressure

P_{LA} Average pressure in the liquid control volume (L)

P_m Local mixture pressure (D)

P_{SA} Average pressure in the steam control volume (L)

Q_{COND} Rate of energy released by the condensing steam at the interface (L)

Q_{EVPR} Rate of energy absorbed by the evaporating liquid at the interface (L)

Q_{HEATR} Actual heat input to the pressurizer fluid from the heaters (L)

Q_{PWR} Electrical power to the heaters (L)

Q_{TR} Heat transfer rate from the liquid control volume to the steam control volume due to the temperature gradient (L)

Q_{WL} Heat loss to the environment through portion of presSUBASH surrounding the liquid control volume (L)

Q_{WS} Heat loss to the environment through portion of pressurizer wall surrounding the steam control volume (L)

q Local conduction heat flux (D)

q^T Local turbulent diffusion flux of energy (D)

q_w'' Local wall heat flux (D)

t Time

T_{LA} Average temperature in the liquid control volume (L)

T_{SA} Average temperature in the steam control volume (L)

V_L Volume of mixture in the liquid control volume (l)

V_S Volume of the mixture in the steam control volume (L)

v_c Local continum phase velocity (D)

v_d Local dispersed phase velocity (D)

v_{dj} Drift velocity (D)

v_f Saturated liquid-phase specific volume

v_g Saturated gas-phase specific volume

v_m Local mixture velocity (D)

W_{BR} Flow of bubbles from the bulk of the liquid control volume rising toward the steam control volume (L)

W_{CD} Flow of condensate droplets from the bulk of the steam control volume toward the liquid volume (L)

W_{CI} Interface condensation rate (L)

W_{EI} Interface evaporation rate (L)

W_{SRL} Surge-line flow (L)

W_{STB} Steam-bleed flow (L)

x Steam quality

x_L Average steam quality in the liquid control volume (L)

x_m Local mixture steam quality (D)

x_S Average steam quality in the steam control volume (L)

z Axial distance (D)

z_{LIQ} Height of the liquid control volume (L)

Greek Symbols

α_c Local continum phase volume fraction (D)

α_d Local dispersed phase volume fraction (D)

α_{gL} Average void fraction in the liquid control volume (L)

β Portion of energy exchange during interface evaporation or condensation that is absorbed or released by the liquid control (L)

Δ_{hdc} Difference between specific enthalpy of the two phases (D)

ΔP Local inter-phase pressure difference (D)

δ Portion of Q_{COND} that is lost to the wall (L)

Γ_d Rate of local interfacial mass transfer for the dispersed phase due to phase change (D)

$\phi_m{}^{\mu}$ Local mixture viscous dissipation term (D)

$\phi_m\sigma$ Work due to surface tension force (D)

$\phi_m i$ Local interfacial mechanical energy transfer term (D)

ρ_c Local continuum phase density (D)

ρ_d Local dispersed phase density (D)

ρ_L Average density of mixture in the liquid control volume (L)

ρ_m Local mixture density (D)

ρ_f Saturated liquid-phase density

ρ_g Saturated gas-phase density

ρ_S Average density of mixture in the steam control volume (L)

τ_{zz} Normal component of mixture viscous stress (D)

$\tau_{zz}{}^T$ Normal component of mixture turbulent stress (D)

ξ_h Heated parameter (D)

Operation Symbols

area average:

$$<F> = \frac{1}{A}\int_A F\,dA$$

phase volume-fraction weight mean value:

$$<<F_k>> = \frac{<\alpha_k F_k>}{<\alpha_k>}$$

mixture average parameter:

$$\overline{\Psi}_m = \frac{[<\alpha_d>\rho_d<<\psi_d>> + (1 - <\alpha_d>)\rho_c<<\psi_c>>]}{<\rho_m>}, \qquad \psi = h, v$$

covariance term:

$$COV(\alpha_k\rho_k\psi_k v_k) = <\alpha_k\rho_k\psi_k(v_k - <<v_k>>)>, \qquad \psi = h, v$$

REFERENCES

1. Gorman, D.J., "Steam Surge Tank Transient During Outsurge", ASME Paper No. 9-WA/NE-14, 1969.

2. Nahavandi, A.N. and Makkenchery, S., "An Improved Pressurizer Model with Bubble Rise and Condensate Drop Dynamics", Nuc. Eng. & Design, Vol. 12, p.135, 1970.

3. Baggoura, B. and Martin, W., "Transient Analysis of the Three Mile Island Unit 2 Pressurizer System", Nuclear Technology, Vol. 62, p.159, 1983.

4. Sami, S.M., "A Dynamic Model for Predicting CANDU Pressurizers Performance", Nuclear Technology, Vol. 72, p.7, 1986.

5. Kim, S.N. and Griffith, P., "PWR Pressurizers Modelling", Proc. of Specialists Meeting on Small Break LOCA Analysis in LWR's, p. 207, 1985.

6. Lin, J.C., Riembe, R.A., Ransom, V.H., and Johnson, G.W., "RELAPS/Mode Pressurizer Modelling", ASME paper No. 84-WA/HT-86.

7. Sollychin, R., Garland, W.J., and Chang, J.S., "The IDRIFF Two-Phase Simulation Code and Its Application to the Study of a Pressurizer", "Multi-phase Transport and Particulate Phenomena", Hemisphere Press, New York (in press 1988).

8. Sollychin, R., Garland, W.J., and Chang, J.S., "Development and Applications of IDRIFF Two-Phase Simulation Code", CNS 12th Symp. Simul. Reac. Dymc. Plant. Contr., Hamilton, Canada, April 1986, Paper No. 2A-1.

9. Sollychin, R., Garland, W.J., and Chang, J.S., "Two-Phase Flow Patterns and Their Transitions in Pressurizers Under Quasi-Steady-State", (to be published).

10. Wulff, W., Cheng, H.S., Mallen, A.N., and Stritar, A., "Kinematics of Two-Phase Mixture Level Motion in BWR Pressure Vessels", Proc. of Specialists Meeting on Small Break LOCA Analysis in LWR's, P. 193, 1985.